

Experimental and Theoretical Studies on the Binding of Epigallocatechin Gallate to Purified Porcine Gastric Mucin

Yanyan Zhao,[†] Longjian Chen,[†] Gleb Yakubov,^{‡,§} Termeh Aminiafshar,^{||} Lujia Han,^{*,†} and Guoping Lian^{*,‡}

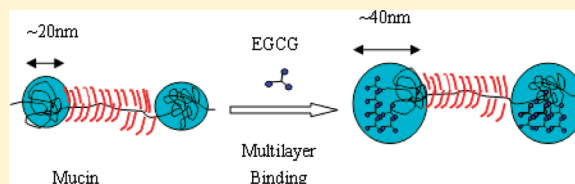
[†]China Agricultural University, Qing-hua-dong-lu, Beijing 100083, P. R. China

[‡]Unilever Research Colworth, Colworth Park, Sharnbrook, Bedford MK44 1LQ, U.K.

[§]Australian Research Council Centre of Excellence in Plant Cell Walls, School of Chemical Engineering, The University of Queensland, Queensland, Australia

^{||}School of Applied Sciences, Cranfield University, Cranfield, Bedfordshire MK43 0AL, U.K.

ABSTRACT: Binding of epigallocatechin gallate (EGCG) to highly purified short side-chain porcine gastric mucin similar to human MUC6 type has been studied by ultraviolet–visible absorption spectroscopy (UV–vis), ultrafiltration isothermal titration microcalorimetry (ITC) and transmission electron microscopy (TEM). The thermodynamic equilibrium of EGCG binding to mucin has been quantitatively determined using ultrafiltration and high-performance liquid chromatography (HPLC)–UV/vis. The relationship suggests multilayer binding rather than simple Langmuir monolayer binding of EGCG. By combining the ultrafiltration and ITC data, the thermodynamic parameters of EGCG binding to mucin have been obtained. The binding constant for the first layer is about an order of magnitude higher than that of the consecutive multilayers. Negative entropy indicates multilayer of EGCG formed. Hydrogen bonding may be responsible for the multilayer formation. Increasing temperature resulted in a decrease in the binding affinity, further suggesting that hydrogen bonds dominated the interaction energy. A TEM micrograph of the EGCG–mucin complex revealed a monodispersion of blobs similar to pure mucin solution but with relatively bigger size (about twice). It is proposed that the EGCG–mucin binding process occurs by single and/or cluster of EGCG molecules driven to the surface of the two hydrophobic globules of mucin by hydrophobic interaction followed by hydrogen bond interaction between EGCG and mucin. Further adsorption of EGCG molecules onto bound EGCG molecules to form multilayers can also occur. This fits well with the observations that EGCG–mucin interaction followed a multilayer adsorption isotherm, the energy released is dominated by hydrogen bonds, and no large aggregates were formed.



INTRODUCTION

Epithelial mucus covers the external surface of mouth, gastric and intestine. Mucin glycoproteins are the major constituents of epithelial mucus.¹ The interaction of saliva mucin with food/drink ingredients has an important effect on flavor and perception. Binding of polyphenols to saliva mucin is believed to be responsible for the sensation of astringency.² Binding of polyphenol compounds to intestinal mucin has an important effect on nutrition and gut health.³ Epigallocatechin gallate (EGCG, Figure 1) is the most abundant polyphenol in green tea and has been associated with many medicinal and health benefits.^{4–7} Interactions of EGCG with food ingredients and biosubstrate proteins have received extensive studies.^{5,8} Studies have been reported on EGCG interaction with bovine serum albumin (BSA),^{9–11} human serum albumin (HSA),^{12–14} proline-rich protein,^{15–17} and bovine mucin.¹⁸ A three-stage polyphenol–protein binding model has been proposed by Charlton et al.¹⁹ for polyphenol binding to proline-rich protein. It was proposed that protein and polyphenols combine to form soluble complexes. Such complexes aggregate to form colloidal particles, which can further lead to sedimentation. Such three

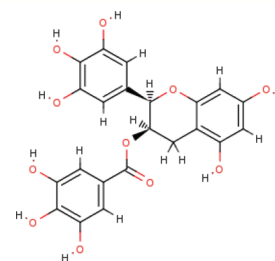


Figure 1. Molecular structure of EGCG.

stage interactions occur in systems such as EGCG and β -casein²⁰ and polyphenol and proline rich peptide.¹⁹ It has been reported that the interaction between polyphenol and glycosylated protein does not follow the three-stage process since the complex formed by polyphenol and glycosylated protein is soluble.¹⁵ Few studies have reported on the

Received: December 14, 2011

Revised: April 10, 2012

Published: April 16, 2012



interaction between polyphenol and glycosylated protein^{15,21,22} but understanding of the interaction is still limited. Pascal, et al.¹⁵ reported the effect of protein glycosylation on the aggregation of proline-rich protein and EGCG. They proposed that the threshold for aggregation must be related to protein concentration as well as to the EGCG/protein ratio. It is still not clear on which site EGCG binds to glycosylated protein and how strong the binding energy is between EGCG and protein. The thermodynamic equilibrium of EGCG binding to glycosylated protein is also not fully understood.

Phenolic compounds can interact with protein via either noncovalent interaction or covalent interaction.²³ Covalent interaction takes place by oxidating the phenolic compounds to radicals and quinones.²³ Very often, phenolic interaction with protein is noncovalent.²⁴ Noncovalent interaction includes electrostatic interaction, van der Waals interaction, hydrogen bonds, hydrophobic interaction, and π bonds. Noncovalent interaction between protein and phenolic compounds can be studied by various techniques such as equilibrium dialysis (ED),^{25,26} ultrafiltration,^{27,28} ultraviolet–visible absorption spectroscopy (UV–vis),^{29,30} fluorescence spectroscopy,^{10,12} capillary electrophoresis,³¹ and isothermal titration microcalorimetry (ITC).^{11,17,32} Using ED and ultrafiltration, the thermodynamic equilibrium of phenolic compounds binding to protein can be determined. However, phenolic compounds can also bind to the membrane used. Furthermore, the ED method is very time-consuming. The spectroscopy method measures the binding affinity in the environment of certain amino acid residues, while the ITC method provides the thermodynamic properties of enthalpy change of the interaction during a titration experiment. By fitting the enthalpy data into a proper binding model, the association constant (K), stoichiometry (n), free energy (G), and enthalpy (H) associated with the interaction can be obtained. However, ITC is a very delicate method and not suitable for both strong and weak interactions.²³

In this paper, various measurement techniques are combined to investigate the binding of EGCG to purified porcine gastric mucin. Highly purified short side-chain porcine gastric mucin similar to human MUC6 type is selected. The mucin used is characterized as a highly glycosylated glycoprotein.^{33–35} Ultrafiltration method has been applied to quantify the thermodynamic equilibrium of EGCG binding to mucin. The associated thermodynamic properties of EGCG binding to mucin including the effect of temperature have been investigated using ITC. The microstructure and properties of the EGCG–mucin complex have been examined by transmission electron microscopy (TEM). The experimental data of ultrafiltration is best fitted by the Guggenheim–Anderson–deBoer (GAB) isotherm model, suggesting multilayer binding of EGCG to mucin. By combining the results of ultrafiltration and ITC, the thermodynamic properties of EGCG binding to mucin have been obtained. A model is proposed to describe the interaction between EGCG and mucin.

MATERIALS AND METHOD

Materials. Water used was filtered tap water using a Milli-Q system (Millipore, Watford, U.K.). EGCG was obtained from Teavigo. The purity was 94%. Mucin was highly purified pharmaceutical-grade porcine gastric “Orthana” mucin purchased from A/S Orthana Kemisk Fabrik (Kastrup, Denmark). Mucin samples were lyophilized and stored at $-20\text{ }^{\circ}\text{C}$ in sealed bottles until use. The purification process and the character-

ization of the purified mucin were reported by Harvey et al.³⁵ previously. This purified mucin was characterized to a molecular weight of 546 kDa measured by static light scattering.³³ It contains 71–76% (weight fraction) sugar, 20–21.5% protein content, and a minute amount of sialic acid.³⁴ There is a relatively high fraction (20–26% weight fraction of overall amino acid) of hydrophobic amino acid (valine, isoleucine, leucine, and alanine) indicating the existence of hydrophobic domains. The existence of polar amino acids of serine and threonine residues provided the sites of O-glycosylation. The O-linked oligosaccharide side chains are composed of predominantly di- and trisaccharides. On the basis of the result of atomic force microscopy (AFM) and TEM experiments, Yakubov et al.³⁴ proposed the monomeric dumbbell-like structure of mucin (Figure 2). These two

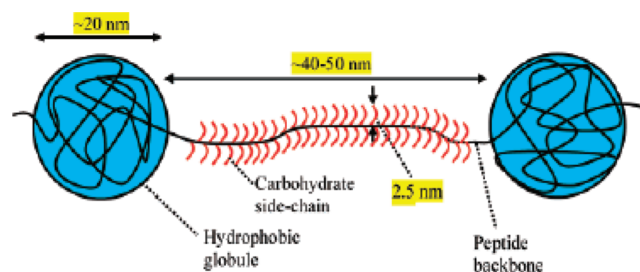


Figure 2. Molecular structure of porcine gastric mucin. The dumbbell-like molecule structure was proposed by Yakubov et al.^{45,46}

globules are formed by hydrophobic domains interaction between the nonglycosylated subunits (hydrophobic and charged amino acids). The two globules are connected by heavily O-glycosylated side chains of sugar groups. The glycosylated side chain of mucin is hydrophilic and allows mucin to be dissolved in water.

Sample Preparation. Mucin solution (9.157×10^{-6} M) was prepared by dissolving 0.1 g lyophilized mucin powder into 20 mL water. Different concentrations of EGCG solution were prepared by dissolving EGCG powder into water and diluting to lower concentrations. Aliquots (2 mL) of the mucin solution (9.157×10^{-6} M) were mixed with EGCG solution (2 mL) at different concentrations. The molar ratio of EGCG to mucin was at 1:1, 5:1, 10:1, 20:1, 50:1, 100:1, 150:1, and 200:1 for the ultrafiltration experiments.

For ITC measurement, mucin solution (9.157×10^{-6} M) was prepared by dissolving mucin in 0.1 M citrate buffer at pH 6. The mucin solution was dialyzed for 12 h against the same dialysis buffer. EGCG solution (2.181×10^{-3} M) was prepared by dissolving in the final buffer used for mucin dialysis.

UV–Vis Measurements. UV–vis spectroscopy measurement was performed on a spectrometer (Lambda 40 UV–vis spectrometer from Perkin-Elmer) at $25\text{ }^{\circ}\text{C}$ in the range of 200–700 nm using a quartz cuvette with 1 cm path length.

EGCG/Mucin Binding Assay. EGCG solutions were mixed with mucin solutions to different molar ratios and incubated for 20 min at $25\text{ }^{\circ}\text{C}$. After incubation, each mixture (4 mL) was placed into an Amicon Ultra-4 centrifugal filter unit, of 3 kDa cutoff (Millipore, Watford, U.K.), and centrifuged at 4000g. Control experiments were carried out for pure EGCG solutions of the same concentration. The amount of bound EGCG was calculated from the concentration difference between the control sample and the filtrate of the test samples.

High-Performance Liquid Chromatography (HPLC). Chromatographic analysis was performed on a Shimadzu HPLC system (Shimadzu, Kyoto, Japan) equipped with SPD-10A UV/vis detector (at 290 nm wavelength). The separation was performed on a Phenomenex column (250 × 4.6 mm ID, 5 μ m) (Macclesfield, Cheshire, UK) using a gradient of aqueous acetic acid (1% in water; solvent A) and acetonitrile with 1% acetic acid (solvent B) at a flow rate of 1.0 mL/min. Chromatography was performed using a linear gradient starting from $t = 0$ min, 10% B and 90% A; $t = 20$ min, 90% B and 10% A; $t = 21$ min, 10% B and 90% A; $t = 30$ min, 10% B and 90% A.

Isothermal Titration Microcalorimetry. An ITC200 titration microcalorimeter (MicroCal, Inc., Northampton, MA) was used at 25, 35, and 45 °C. Protein solution was placed in the 200 μ L sample cell, and EGCG solution was loaded into the injection syringe. Both solutions were degassed before each titration. The duration of each injection was 5 s, and the time interval between injections was 180 s. The solution in the cell was stirred at 500 rpm by the syringe to ensure thorough mixing. Control experiments were also carried out for the titration of EGCG solution into buffer and buffer into the mucin solution. The heat of the control experiments was subtracted from the titration experiment of EGCG and mucin titration, to remove the association and dilution effect.

TEM Study of EGCG and Mucin Solution Mixture. TEM measurements were performed with a JEOL JEM-1200 EX II microscopy. A solution mixture of total EGCG and mucin (1 mg/mL) at molar ratio of 50:1 was negatively stained onto a plasma-treated, carbon-coated, hydrophilic grid.

RESULTS AND DISCUSSION

UV–Vis Absorption Spectroscopy. Figure 3 shows the absorption spectra of EGCG solution only (the dotted line)

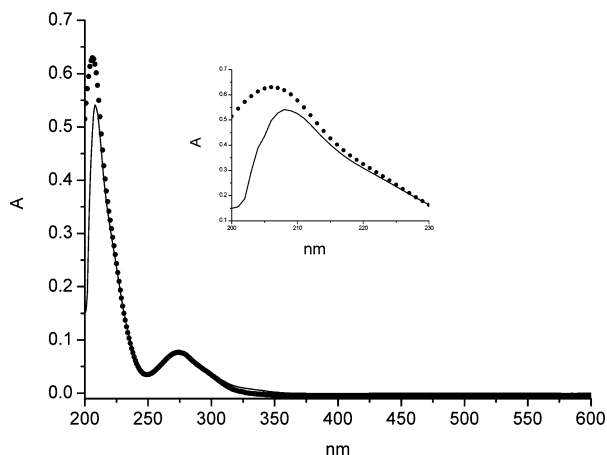


Figure 3. UV–vis spectra of EGCG (dotted line) and EGCG–mucin mixture (20:1) after subtracting the spectra of mucin only (solid line).

and the solution mixture of EGCG and mucin at 20:1 molar ratio after subtracting the spectra of mucin solution (the solid line). UV–vis spectra of EGCG reveal strong absorptions at λ 273 nm and 206 nm. The peak maximum at approximately 206 and 273 nm corresponds to the carbonyl group and benzene ring in the structure of EGCG. There is a difference in the absorption spectrum at 206 nm peak between the EGCG solution and the EGCG–mucin solution mixture after subtracting mucin solution at the same concentration. The

absorption peak not only decreased but also blue-shifted, indicating that the carbonyl group of EGCG is involved in the interaction, but the absorption peak at 273 nm did not change noticeably. In the study of Diniz et al.,³⁶ it was pointed out that the presence of the carbonyl group in the structure of polyphenol is related to the binding to human serum proteins. This is supported by the UV–vis result that the absorption peak of the carbonyl group of EGCG decreased after mixing with mucin. On the other hand, EGCG is a relatively hydrophobic (nonpolar) molecule, and the hydrophobic interaction with the solvent should favor the binding of EGCG to the hydrophobic surface of the two globules of mucin. Thus we can infer that both the hydrogen bond and the hydrophobic interaction are involved in EGCG binding to mucin.

EGCG/Mucin Binding Assay. Binding of EGCG to mucin leads to a reduction of free EGCG concentration in a EGCG–mucin solution mixture. Incubated EGCG–mucin solution mixture and EGCG solution only (control) were ultrafiltrated in a centrifugal filter unit. The difference in the measured EGCG concentration between the EGCG–mucin solution mixture and control sample provides a measure of the EGCG bound to mucin. Ultrafiltration measurements have been carried out for different EGCG–mucin ratios to obtain the binding isotherm. The results are shown in Figure 4.

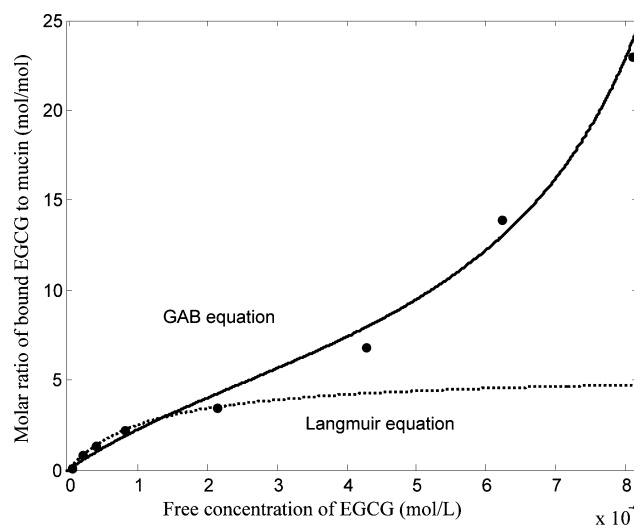


Figure 4. Ultrafiltration data of EGCG–mucin isotherm measured by ultrafiltration. Data is best fitted by eq 1.

In many studies, the Langmuir isotherm was used to describe ligand–protein binding equilibrium.^{37,38} However, the Langmuir isotherm applies to monolayer adsorption, and the ligand binding reaches a maximum as the ligand-to-protein ratio increases. As it is shown in Figure 4, this is not the case for EGCG–mucin binding, suggesting multilayer binding equilibrium. The BET isotherm model developed by Brunauer, Emmett, and Teller³⁹ is usually used to describe multilayer adsorption. For liquid phase adsorption, the BET equation is further modified in the following form (also known as the GAB equation):^{40,41}

$$q = q_m \frac{K_s C_{eq}}{(1 - K_L C_{eq})(1 - K_L C_{eq} + K_s C_{eq})} \quad (1)$$

where q is the amount of ligand bound per mole protein (mol/mol), C_{eq} is the free ligand concentration (M), q_m is the amount of monolayer binding of ligand per mol protein (mol/mol), K_S is the monolayer binding constant (M^{-1}), and K_L is the multilayer binding constant (M^{-1}).

Figure 4 shows that the experimental data of EGCG binding to mucin is best fitted by the GAB isotherm. Fitted GAB parameters of q_m , K_S , and K_L are listed in Table 1. For comparison, the Langmuir isotherm is also shown in Figure 4.

Table 1. Fitted Isotherm Parameters of EGCG–Mucin Binding

	GAB	Langmuir
K_S	4343	8658
K_L	927.8	—
q_m	6.342	5.414
R^2	0.9920	0.2467

Schwarz and Hofman²⁷ reported that EGCG binding to salivary protein (nonglycosylated protein) reaches a maximum plateau as the molar ratio of EGCG to protein increases. The result of the current study suggests that EGCG binding to mucin does not have such a maximum. One characteristic of EGCGs in solution is that they tend to self-associate due to hydrophobic interaction between the aromatic ring and hydrogen bonding between hydroxyl groups.^{19,42} It is very likely that there are cooperative multiple EGCGs binding to mucin competing with EGCG–EGCG interaction. For nonglycosylated protein, EGCGs could easily bind to the hydrophobic peptide of the protein. By increasing EGCG concentration, the interaction of EGCG self-association increases as well. This leads to cross-linking between different protein molecules, causing insolubility and precipitation. With precipitation occurring, the amount of EGCG bound to nonglycosylated protein reaches a fixed level of maximum. This is apparently not the case for the interaction between EGCG and glycosylated protein. Because of the location of glycosyl moieties, the protein bridging of EGCG cannot be formed, and the complex is still soluble. This is supported by the ultrafiltration experimental data where the amount of EGCG bound to mucin increases as the molar ratio of EGCG to mucin increases.

Thermodynamic Properties of EGCG–Mucin Binding.

ITC data of EGCG–mucin binding are obtained as a plot of heat flux against time. The data are integrated peak-by-peak and normalized to obtain the enthalpy change per mole of injectant (ΔH , kJ/mol) against the molar ratio (EGCG/mucin). Figure 5 shows the results of titration of EGCG (2.181×10^{-3} M, at pH 6, 25 °C) into mucin (9.157×10^{-6} M, at pH 6, 25 °C). Usually, the control experiment for injection of a ligand into buffer will consist of a series of equal heats of dilution.⁴³ EGCG tends to self-associate due to its hydrophobicity.⁴⁴ Therefore, when injected into the buffer, EGCG undergoes an endothermic process of disaggregation. The interaction between EGCG and mucin is exothermic. To obtain the heat changes due to the binding of EGCG to mucin, the heat of the control experiment is subtracted from that of titration experiment of EGCG to mucin. The final experimental results are represented by the normalized enthalpy change developed versus the cell total ligand to protein ratio as shown in Figure 5. The measured values of the enthalpy changes of the interaction

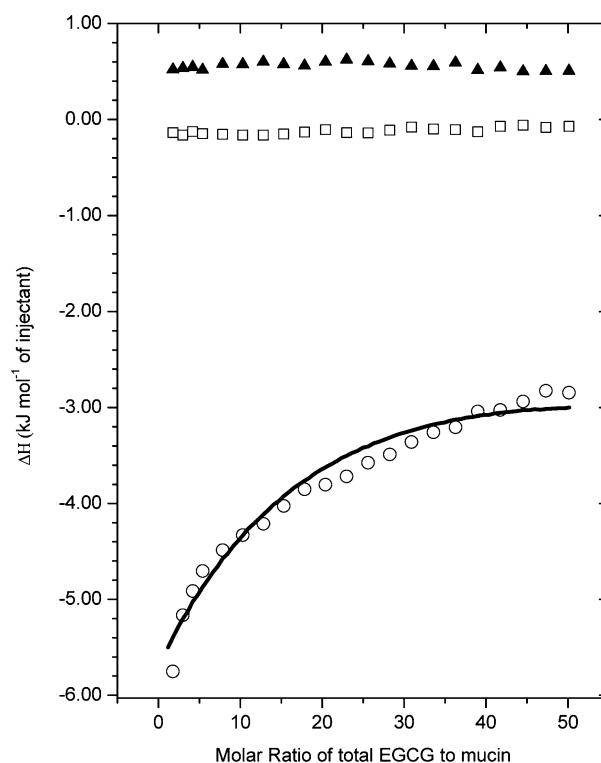


Figure 5. ITC data of EGCG (2.181×10^{-3} M, at pH 6, 25 °C) titration to mucin (9.157×10^{-6} M, at pH 6, 25 °C). Molar enthalpy change (ΔH , kJ/mol) against the molar ratio of the total EGCG to mucin after subtracting the control experiment. \blacktriangle : the control experiment of EGCG titration into empty buffer; \square : the control experiment of citrate buffer titration into mucin solution; \circ : observed enthalpy changes of EGCG and mucin after subtracting the control experiment. The solid line is the fitted enthalpy changes using the GAB binding adsorption isotherm model.

are relatively small, suggesting that the interaction of EGCG with mucin is a relatively weak binding.⁴³

The measured enthalpy change data can be fitted to theoretical ligand-binding models to further obtain the thermodynamic parameters of the interaction. Use of the Langmuir isotherm model did not produce a good fit of the data, which further confirmed that the binding of EGCG to mucin is not a simple monolayer. One of the difficulties in fitting ITC data to more complex binding models is the increase of the number of fitted parameters. Overparameterization often leads to multiple solutions of local minima, causing uncertainties in the thermodynamic properties. Here, in order to reduce such uncertainty, the GAB binding isotherm of eq 1 derived from the ultrafiltration is used to reduce the number of fitted parameters. With the GAB binding isotherm, the total heat Q can be decomposed into two components, including the heat associated with the monolayer binding and that with the multilayer binding.

$$Q = Q_{\text{mono}} + Q_{\text{multi}} \quad (2)$$

where Q_{mono} is the heat of the first layer binding of EGCG to mucin, and Q_{multi} is the heat of the consecutive layers.

The amount of the first layer binding of EGCG to mucin can be derived from the following Langmuir equation:

$$M_{\text{mono}} = M_t V \times q_m \frac{K_S C_{eq}}{(1 + K_S C_{eq})} \quad (3)$$

Table 2. Thermodynamic Parameters of EGCG Binding to Mucin at Different Temperatures of 25, 35, and 45 °C^a

temperature(°C)	q_m	K_S	K_L	ΔH_1 (kJ/mol)	ΔH_2 (kJ/mol)	ΔG_1 (kJ/mol)	ΔG_2 (kJ/mol)	ΔS_1 (J/mol/K)	ΔS_2 (J/mol/K)	R^2
25	6.342	4343	927.8	-27.96	-33.27	-20.75	-16.93	-24.19	-54.83	0.9718
35	6.209	3019	787.0	-24.20	-32.77	-20.52	-17.08	-11.95	-50.94	0.9980
45	6.423	2167	553.7	-23.07	-32.77	-20.31	-16.70	-8.679	-50.53	0.9994

^aData obtained by fitting to ITC data using the GAB binding isotherm.

The amount of the consecutive multilayer binding of EGCG to mucin is thus given as

$$M_{\text{multi}} = M_t V \times \left[q_m \frac{K_S C_{\text{eq}}}{(1 - K_L C_{\text{eq}})(1 - K_L C_{\text{eq}} + K_S C_{\text{eq}})} - q_m \frac{K_S C_{\text{eq}}}{(1 + K_S C_{\text{eq}})} \right] \quad (4)$$

It follows that the total heat for binding of the first-layer and consecutive layers of EGCG is

$$Q = M_t V \left\{ q_m \frac{K_S C_{\text{eq}}}{(1 + K_S C_{\text{eq}})} \Delta H_1 + \left[q_m \frac{K_S C_{\text{eq}}}{(1 - K_L C_{\text{eq}})(1 - K_L C_{\text{eq}} + K_S C_{\text{eq}})} - q_m \frac{K_S C_{\text{eq}}}{(1 + K_S C_{\text{eq}})} \right] \Delta H_2 \right\} \quad (5)$$

Here M_t is the bulk concentration of mucin in the cell. ΔH_1 and ΔH_2 are the molar heats of EGCG–mucin interaction of the first and consecutive layers, respectively. V is the cell volume (200 μL). C_{eq} is the concentration of free ligand, which is calculated from the total EGCG concentration and the bound EGCG concentration in the cell as follows:

$$X_t = C_{\text{eq}} + M_t q_m \frac{K_S C_{\text{eq}}}{(1 - K_L C_{\text{eq}})(1 - K_L C_{\text{eq}} + K_S C_{\text{eq}})} \quad (6)$$

where X_t is the overall concentration of EGCG in the cell. Both X_t and M_t are obtained from ITC experimental data.

The measured enthalpy change of each injectant is

$$\Delta H = \left(Q(i) - Q(i-1) + \frac{dV_i}{V} \left(\frac{Q(i) - Q(i-1)}{2} \right) \right) / (C_{\text{egcg}} \times dV_i) \quad (7)$$

where C_{egcg} is the concentration of EGCG in the syringe ($2.181 \times 10^{-3} \text{ M}$), and dV_i is the injection volume for the i th injection.

In eqs 5–7, there are only two unknown parameters of ΔH_1 and ΔH_2 . Fitting eqs 5–7 to the experimentally measured data of ΔH produces the values of the unknown parameters of ΔH_1 and ΔH_2 as listed in Table 2. The free energy of EGCG–mucin interaction of the first and consecutive layers ΔG_1 and ΔG_2 are obtained by

$$\Delta G_1 = -RT \ln K_S \quad (8)$$

$$\Delta G_2 = -RT \ln K_L \quad (9)$$

where R is the universal gas constant (8.314 J/mol/K), and T is temperature (K).

The adsorption entropy ΔS_1 and ΔS_2 are easily calculated by

$$\Delta S_1 = \frac{\Delta H_1 - \Delta G_1}{T} \quad (10)$$

$$\Delta S_2 = \frac{\Delta H_2 - \Delta G_2}{T} \quad (11)$$

The binding constant for the monolayer is about an order of magnitude higher than that of the consecutive multilayer. The negative entropy (ΔS) indicates an increase in molecular order.⁹ This suggests that hydrogen bond interactions play a role in the formation of complex and also EGCG–EGCG multilayer aggregation occurs.^{9,44} Figure 5 also shows that the modified isotherm model fits well to the ITC data.

Figure 6 summarizes the ITC results of EGCG solution titrated into mucin solution at 25, 35, and 45 °C. Increasing

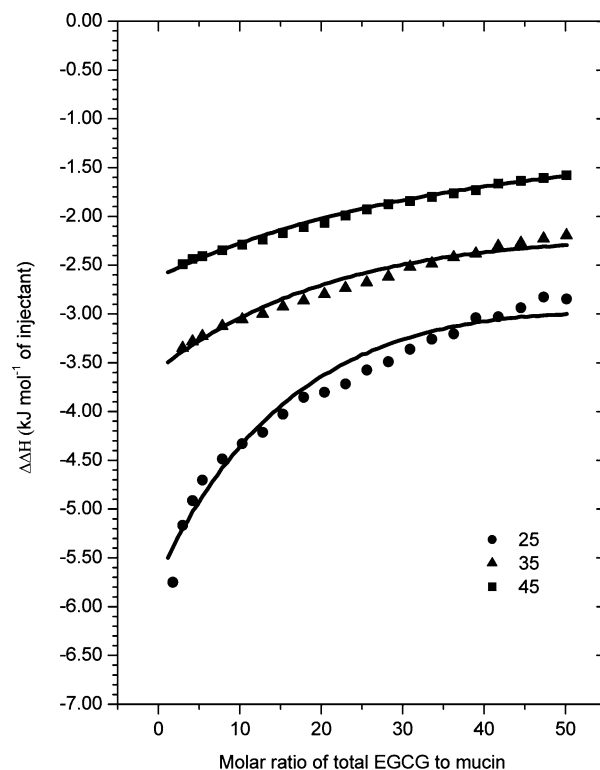


Figure 6. Molar enthalpy change (ΔH , kJ/mol) against the molar ratio of total EGCG ($2.181 \times 10^{-3} \text{ M}$) to mucin ($9.157 \times 10^{-6} \text{ M}$) after subtracting the control experiment at pH 6, 25, 35, and 45 °C. The solid line is the fitted enthalpy changes using the GAB binding isotherm model.

temperature causes a diminished release of the binding energy. The GAB isotherm model was also chosen to fit the ITC data at 35 and 45 °C. Table 2 shows the fitted binding thermodynamic parameters at different temperatures. The values of K_S and K_L decreased with increasing temperature. The derived binding enthalpies are typical values of non-covalent interaction and much lower than that of covalent bond

formation (200–400 kJ/mol).⁹ For polyphenol binding to protein, hydrogen bonding and hydrophobic interaction are believed to be the main driving forces,²³ but the extent and relative importance of them are controversial.⁴⁵ The temperature effect on the binding energy associated with hydrogen bonding is opposite that of hydrophobic interaction. Increasing temperature causes a decrease in the binding energy of hydrogen bonding but an increase in the binding energy of hydrophobic interaction.²³ That the measured binding energy released decreases with increasing temperature suggests that the energy associated with hydrogen bonding dominates, and that associated with the hydrophobic interaction is relatively small. However, this does not exclude the existence of hydrophobic interaction in EGCG–mucin binding. Ross et al.⁴⁶ suggested a two-step process of protein–ligand binding, consisting of two hydrophobic parts coming into proximity by hydrophobic interaction and further intermolecular interactions involving ionic interaction, hydrogen bonds, and van der Waals interactions. It appears that EGCG binding to mucin is initiated by hydrophobic interaction followed by hydrogen bond interaction.

TEM Micrograph and Size Distribution of EGCG and Mucin Solution Mixture. No sedimentation was observed for the EGCG–mucin solution mixtures studied. TEM micrographs were obtained, and Figure 7a shows the polydisperse nature present in the EGCG/mucin solution mixture. Unlike the EGCG/ β -casein solution mixture studied by Jobstl et al.,²⁰

there are no large aggregates present for the EGCG–mucin system. The glycosyl moieties of heavily glycosylated mucin are strongly hydrophilic and must remain exposed to the aqueous phase. This explains why there are no large aggregates.¹⁵ Yakubov et al.^{33,34} reported the phase images of mucin solution at a concentration of 1 mg/mL and observed a blob radius of a typical mucin blob between 6 and 10 nm. Here, the TEM micrograph of the EGCG–mucin mixture (1 mg/mL mucin and EGCG/mucin molar ratio of 50:1) showed slightly bigger sizes of blobs, as shown in Figure 7. The majority of the values of the blob radius are in the range of 12–20 nm. We infer that binding of EGCG to mucin is primarily at the hydrophobic heads, which will cause some expansion in size, but will unlikely extend to such. Further investigation would be needed.

Molecular model for EGCG–mucin interaction. Previously, a three-stage model was suggested for polyphenol binding to proline-rich protein¹⁹ and β -casein.²⁰ The proposed three stages are the formation of a soluble complex of protein and polyphenols, growth of aggregates, and sedimentation. Compared to proline-rich protein and β -casein, mucin is made of highly glycosylated macromolecules (50–80% by weight).³³ The protein backbone of mucin is characterized by numerous tandem repeats that contain proline and are high in serine and threonine residues. Numerous *O*-glycans are attached to threonine or serine residues in the tandem repeat domains.¹ The glycosyl moieties are strongly hydrophilic. The glycosylation creates steric hindrance that limits the extent of EGCG binding to the hydrophobic amino residues at the backbone of mucin. On the other hand, exposed amino acids such as valine, isoleucine, and leucine at the hydrophobic head can interact with EGCG via a hydrogen bond with a location advantage. Here the model of mucin and EGCG binding is proposed as clusters of EGCG molecules bound to the hydrophobic head of mucin via hydrogen bond interaction and further EGCG self-association to bound EGCG, leading to multilayer adsorption. The consequences are that (a) hydrogen bonds dominate the binding energy, (b) the thermodynamic equilibrium of binding follows a multilayer adsorption isotherm, and (c) aggregation to form large particles by cross-linking did not occur, hence the EGCG–mucin complex remains soluble. This indeed appears to be supported by our experimental observations.

CONCLUSION

EGCG binding to mucin has been investigated by a combination of techniques of UV–vis absorption spectroscopy, ultrafiltration, TEM, and ITC. The UV–vis result supports that the carbonyl group present in the structure of EGCG is involved in the binding to mucin. Further NMR and IR studies could confirm this. The thermodynamic equilibrium of EGCG binding to mucin was determined by ultrafiltration, and the data is best fitted by GAB isotherm, suggesting multilayer EGCG binding to mucin rather than simple monolayer binding. The thermodynamic property of EGCG binding to mucin has been further characterized by ITC. The recorded enthalpy for EGCG–mucin binding is relatively low. The binding constant for the first layer is about an order of magnitude higher than the multilayers. Negative entropy indicates that a multilayer of EGCG formed during the binding process and also implies hydrogen bonding in the formation of the complex EGCG–mucin. Increasing temperature causes a decrease in the binding energy. This is a typical behavior of hydrogen bonds, further suggesting that the energy released during EGCG–mucin binding is dominated by that of hydrogen bonds. A TEM

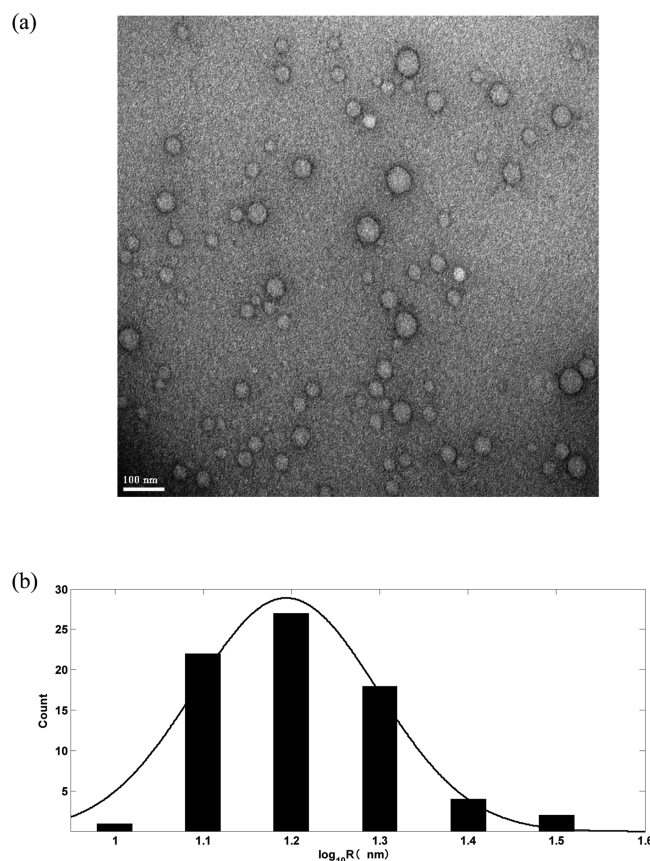


Figure 7. (a) TEM micrograph of a EGCG–mucin mixture at a molar ratio of 50:1. The concentration of mucin is 1 mg/mL. A hydrophilic carbon film is used. (b) Size distribution histogram of the mucin and EGCG mixture.

micrograph of the EGCG–mucin complex exhibited a similar monodispersion of blobs of the mucin-only system reported before,^{33–35} but about twice larger in radius. It appears that EGCG–mucin binding follows the steps of single and/or a cluster of a few EGCG molecules driven to the proximity of the hydrophobic heads of mucin by hydrophobic interaction at a molecular level followed by hydrogen bond interaction between EGCG and mucin at an atomic level. Free EGCG molecules can be also adsorbed onto already bound EGCG molecules to form multilayers.

AUTHOR INFORMATION

Corresponding Author

*(L.H.) Address: College of Engineering, China Agricultural University (East Campus), Beijing 100083, China; e-mail: hanlj@cau.edu.cn. (G.L.) Address: Unilever Research, Colworth, Sharnbrook, Bedford MK44 1LQ, U.K.; e-mail: guoping.lian@unilever.com.

Notes

The authors declare no competing financial interest.

ACKNOWLEDGMENTS

This research is financially supported by Unilever R&D Colworth and the National Natural Science Foundation of China (Project No. 21006124). Y.Z. wishes to thank Derek Atkins for his assistance with TEM measurement.

REFERENCES

- (1) Rose, M. C.; Voynow, J. A. *Physiol. Rev.* **2006**, *86*, 245–278.
- (2) Rossetti, D.; Yakubov, G. E.; Stokes, J. R.; Williamson, A. M.; Fuller, G. G. *Food Hydrocolloids* **2008**, *22*, 1068–1078.
- (3) Baxter, N. J.; Lilley, T. H.; Haslam, E.; Williamson, M. P. *Biochemistry* **1997**, *36*, 5566–5577.
- (4) Adhami, V. M.; Mukhtar, H. *Mol. Biotechnol.* **2007**, *37*, 52–57.
- (5) Ripley, B. J. M.; Fujimoto, M.; Serada, S.; Ohkawara, T.; Nishikawa, T.; Terabe, F.; Matsukawa, Y.; Stephanou, A.; Knight, R. A.; Isenberg, D. A.; et al. *Int. Immunol.* **2010**, *22*, 359–366.
- (6) Lambert, J. D.; Sang, S.; Hong, J.; Yang, C. S. *J. Agric. Food Chem.* **2010**, *58*, 10016–10019.
- (7) Magrone, T.; Jirillo, E. *Curr. Med. Chem.* **2011**, *11*, 1780–1796.
- (8) Chow, H. H. S.; Cai, Y.; Alberts, D. S.; Hakim, I.; Dorr, R.; Shahi, F.; Crowell, J. A.; Yang, C. S.; Hara, Y. *Cancer Epidemiol., Biomarkers Prev.* **2001**, *10*, 53–58.
- (9) Frazier, R. A.; Papadopolou, A.; Green, R. J. *J. Pharm. Biomed. Anal.* **2006**, *41*, 1602–1605.
- (10) Soares, S.; Mateus, N.; De Freitas, V. *J. Agric. Food Chem.* **2007**, *55*, 6726–6735.
- (11) Xi, J.; Fan, L. *J. Therm. Anal. Calorim.* **2010**, *102*, 217–223.
- (12) Dufour, C.; Dangles, O. *Biochem. Biophys. Acta, Gen. Subj.* **2005**, *1721*, 164–173.
- (13) Bolli, A.; Marino, M.; Rimbach, G.; Fanali, G.; Fasano, M.; Ascenzi, P. *Biochem. Biophys. Res. Commun.* **2010**, *398*, 444–449.
- (14) Ishii, T.; Minoda, K.; Bae, M. J.; Mori, T.; Uekusa, Y.; Ichikawa, T.; Aihara, Y.; Furuta, T.; Wakimoto, T.; Kan, T.; et al. *Mol. Nutr. Food Res.* **2010**, *54*, 816–822.
- (15) Pascal, C.; Poncet-Legrand, C.; Cabane, B.; Vernhet, A. *J. Agric. Food Chem.* **2008**, *56*, 6724–6732.
- (16) Pascal, C.; Poncet-Legrand, C.; Imbert, A.; Gautier, C.; Sarni-Manchado, P.; Cheynier, V.; Vernhet, A. *J. Agric. Food Chem.* **2007**, *55*, 4895–4901.
- (17) Poncet-Legrand, C.; Gautier, C.; Cheynier, V.; Imbert, A. *J. Agric. Food Chem.* **2007**, *55*, 9235–9240.
- (18) Monteleone, E.; Condelli, N.; Dinnella, C.; Bertuccioli, M. *Food Qual. Prefer.* **2004**, *15*, 761–769.
- (19) Charlton, A. J.; Baxter, N. J.; Khan, M. L.; Moir, A. J. G.; Haslam, E.; Davies, A. P.; Williamson, M. P. *J. Agric. Food Chem.* **2002**, *50*, 1593–1601.
- (20) Jöbstl, E.; O'Connell, J.; Fairclough, J. P. A.; Williamson, M. P. *Biomacromolecules* **2004**, *5*, 942–949.
- (21) Lu, Y.; Bennick, A. *Arch. Oral Biol.* **1998**, *43*, 717–728.
- (22) Bacon, J. R.; Rhodes, M. J. C. *J. Agric. Food Chem.* **2000**, *48*, 838–843.
- (23) Prigent, S. V. E., Thesis, University of Wageningen, Wageningen, The Netherlands, 2005.
- (24) Wiese, S.; Gärtner, S.; Rawel, H. M.; Winterhalter, P.; Kulling, S. E. *J. Sci. Food Agric.* **2009**, *89*, 33–40.
- (25) Pablo Villamor, J.; Zátón, A. M. L. *J. Biochem. Biophys. Methods* **2001**, *48*, 33–41.
- (26) Feldman, K. S.; Sambandam, A.; Lemon, S. T.; Nicewonger, R. B.; Long, G. S.; Battaglia, D. F.; Ensel, S. M.; Laci, M. A. *Phytochemistry* **1999**, *51*, 867–872.
- (27) Schwarz, B.; Hofmann, T. *Eur. Food Res. Technol.* **2008**, *227*, 1693–1698.
- (28) Wang, L.; Ren, J. G. *Chin. Pharm. J.* **2008**, *43*, 1579–1581.
- (29) Karnaukhova, E. *Biochem. Pharmacol.* **2007**, *73*, 901–910.
- (30) Zhang, W.; Han, B.; Zhao, S.; Ge, F.; Xiong, X.; Chen, D.; Liu, D.; Chen, C. *Anal. Lett.* **2010**, *43*, 289–299.
- (31) Knjazeva, T.; Kaljurand, M. *Anal. Bioanal. Chem.* **2010**, *397*, 2211–2219.
- (32) McRae, J. M.; Falconer, R. J.; Kennedy, J. A. *J. Agric. Food Chem.* **2010**, *58*, 12510–12518.
- (33) Yakubov, G. E.; Papagiannopoulos, A.; Rat, E.; Easton, R. L.; Waigh, T. A. *Biomacromolecules* **2007**, *8*, 3467–3477.
- (34) Yakubov, G. E.; Papagiannopoulos, A.; Rat, E.; Waigh, T. A. *Biomacromolecules* **2007**, *8*, 3791–3799.
- (35) Harvey, N. M.; Yakubov, G. E.; Stokes, J. R.; Klein, J. *Biomacromolecules* **2011**, *12*, 1041–1050.
- (36) Diniz, A.; Escuder-Gilbert, L.; Lopes, N. P.; Villanueva-Camañas, R. M.; Sagrado, S.; Medina-Hernández, M. J. *Anal. Bioanal. Chem.* **2008**, *391*, 625–632.
- (37) Ku, C. S.; Sathishkumar, M.; Mun, S. P. *Chemosphere* **2007**, *67*, 1618–1627.
- (38) Chitpan, M.; Wang, X.; Ho, C. T.; Huang, Q. *J. Agric. Food Chem.* **2007**, *55*, 10110–10116.
- (39) Brunauer, S.; Emmett, P. H.; Teller, E. *J. Am. Chem. Soc.* **1938**, *60*, 309–319.
- (40) Ebadi, A.; Soltan Mohammadzadeh, J. S.; Khudiev, A. *Adsorption* **2009**, *15*, 65–73.
- (41) Anderson, R. B. *J. Am. Chem. Soc.* **1946**, *68*, 686.
- (42) Wróblewski, K.; Muhandiram, R.; Chakrabarty, A.; Bennick, A. *Eur. J. Biochem.* **2001**, *268*, 4384–4397.
- (43) Turnbull, W. B.; Daranas, A. H. *J. Am. Chem. Soc.* **2003**, *125*, 14859–14866.
- (44) Frazier, R. A.; Deaville, E. R.; Green, R. J.; Stringano, E.; Willoughby, I.; Plant, J.; Mueller-Harvey, I. *J. Pharm. Biomed. Anal.* **2010**, *51*, 490–495.
- (45) Wang, S. H.; Liu, F. F.; Dong, X. Y.; Sun, Y. *J. Phys. Chem. B* **2010**, *114*, 11576–11583.
- (46) Ross, P. D.; Subramanian, S. *Biochemistry* **1981**, *20*, 3096–3102.

NOTE ADDED AFTER ASAP PUBLICATION

This paper was published on the Web on April 23, 2012. The original authorship list was corrected to acknowledge the appropriate author contributions. Please see DOI: 10.1021/jp309790q for more details. The corrected version was reposted on October 18, 2012.